Available online at www.sciencedirect.com
SCIENCE DIRECT®
Biochemical and Biophysical Research Communications 327 (2005) 300–305
BBRC
www.elsevier.com/locate/ybbrc

Characterization of newly cloned variant of rat glycine receptor α1 subunit

Koichi Inoue[a,*], Shinya Ueno[a], Junko Yamada[b], Atsuo Fukuda[a,b]

[a] Department of Physiology, Hamamatsu University School of Medicine, Hamamatsu, Shizuoka 431-3192, Japan
[b] Department of Biological Information Processing, Graduate School of Electronic Science and Technology, Shizuoka University, Hamamatsu, Shizuoka 432-8011, Japan

Received 28 November 2004
Available online 18 December 2004

Abstract

Responses to glycine, a major inhibitory neurotransmitter within the nervous system, are mediated by glycine receptors (GlyRs). Here, we report the cloning and analysis of a novel splicing variant of the GlyRα1 subunit. This variant, named GlyRα1^{del}, has a truncated cytoplasmic region between transmembrane domains (TM)3 and TM4, and compared to other variants, the truncation is contributed by a different acceptor site in exon 9. We transfected GlyRα1 or GlyRα1^{del} into HEK293 cells, and then examined the glycine-activated currents using a whole-cell patch-clamp recording technique. Maximal currents and current–voltage relationships showed no clear difference between GlyRα1^{del} and GlyRα1. Moreover, dose–response curves indicated that the EC_{50} values for glycine differed significantly between the two GlyRα1 derivatives, although their Hill coefficients were similar. When present with other isoforms, GlyRα1^{del} might alter the response to glycine or to other agonists, as this variant expands the potential heterogeneity among glycine receptors.

Keywords: Glycine receptor; Cloning; Alternative splicing; Electrophysiology; Brain; Rat

Glycine, a major inhibitory neurotransmitter within the mammalian central nervous system, targets glycine receptors (GlyRs). The GlyRs are examples of ligand-gated ion channels that conduct Cl^- ions and mediate fast inhibition [1,2]. In general, GlyRs are presumed to form heteromeric pentamers consisting of three α subunits and two β subunits. The α subunits exist in three isoforms with different primary sequences and different developmental expression patterns in the rat brain, expression of the α2 subunit being predominantly embryonic while those of the α1 and α3 subunits (GlyRα1 or GlyRα3, respectively) increase with postnatal development [3–5]. The α1 subunit has been well characterized because of its involvement in human startle disease, hyperekplexia [6–8]. Like other ligand-gated ion channels, GlyRα1 has four transmembrane domains, TM1–TM4. Commonly, such ligand-gated ion channels have a short intracellular loop between TM1 and TM2, while the cytoplasmic loop between TM3 and TM4 is relatively long. For some ligand-gated ion channels, the latter region has been shown to contain elements involved in the recognition and binding of various cytoplasmic proteins and cytoskeleton-linking elements (e.g., acetylcholine receptors interact with rapsyn [9,10], a cytoskeleton-binding element, whereas GlyRβ bind the tubulin-binding protein, gephyrin [11]). In several other ligand-gated ion channels, this region contains modulatory sites [1,12]. The above reports imply that the intracellular loop between TM3 and TM4 is important for channel function.

In this study, we report the cloning of rat GlyRα1^{del}, a novel isoform of GlyRα1, which by comparison with

* Corresponding author. Fax: +8153 435 2245.
E-mail address: inok@hama-med.ac.jp (K. Inoue).

0006-291X/$ - see front matter © 2004 Elsevier Inc. All rights reserved.
doi:10.1016/j.bbrc.2004.12.010

the wild-type receptor, has a different acceptor site in exon 9 with a 90 bp deletion, resulting in a 30 a.a. deletion within the cytoplasmic region between TM3 and TM4. Our functional characterization of this receptor revealed some alterations in pharmacological properties, and so to distinguish the mutant GlyRα1 from the wild-type receptor, we term the latter "GlyRα1WT."

Materials and methods

Cloning and plasmid construction. The total cellular RNA from adult male Sprague–Dawley rat whole brains was obtained using Isogen (Nippongene) according to the manufacturer's protocols. Single-strand cDNA synthesis was then performed using Superscript II (Invitrogen) according to the manufacturer's protocols. The polymerase chain reaction (PCR) was performed to obtain full-length rat GlyRα1 using two oligonucleotide primers (forward: 5′-ggggaattcatg tacagcttcaacactctg-3′, reverse: 5′-gggctcgagtcacttgttgtggacgtcctct-3′), with the above cDNA as a template. The PCR products were electrophoresed, purified, and cloned into the pGEM-T vector (Promega). The nucleotide sequences of these PCR products were determined using an ABI 3100 (Applied Biosystems).

The *Eco*RI–*Xho*I fragments of GlyRα1WT and GlyRα1^{del} were subcloned into both pCMV-Tag2B (Stratagene) and pCDNA3 (Invitrogen).

Cell cultures and transient transfection. HEK293 and COS-7 cells were maintained in Dulbecco's minimum essential medium (Sigma) supplemented with 10% fetal bovine serum at 37 °C in a CO_2 incubator. Cells grown on 35-mm culture plates were transfected using Lipofectamine (Invitrogen) with 0.9 μg of each cDNA. Simultaneous cotransfection of 0.1 μg of enhanced green fluorescent protein (EGFP; Clontech) or CD8 reporter cDNA was performed to enable detection of transfected cells at the time of electrophysiological recording. EGFP-positive cells were visually identified using a fluorescence microscope (ECLIPSE E600FN; Nikon), and CD8-positive cells were identified following brief incubation with microspheres coated with an antibody against CD8 antigen (Dynal Biotech).

Immunoblotting. Samples were resolved by sodium dodecyl sulfate (SDS)–polyacrylamide gel electrophoresis (PAGE), followed by electrotransfer to polyvinylidene difluoride membranes. For visualization, blots were probed with anti-Flag antibody (Sigma), and detected using horseradish peroxidase-conjugated secondary antibody (Bio-Rad) and an ECL kit (Amersham–Pharmacia Biotech).

Immunofluorescence staining. Transfected cells on coverslips were fixed using 4% paraformaldehyde in phosphate-buffered saline (PBS), followed by permeation in PBS containing 0.2% Triton X-100. The cells were then incubated first with anti-Flag antibody and then with Texas red-conjugated secondary antibody (Molecular Probes). For DNA staining, cells on coverslips were incubated with 1 μg/ml of 4′,6-diamidino-2-phenylindole (DAPI) (Sigma). Fluorescent images were analyzed using fluorescence microscopy.

Electrophysiological measurements. Whole-cell recordings were obtained from HEK293 cells 2–3 days after transfection. The preparation was continuously superfused (~1 ml/min) at room temperature (22–25 °C) with an external solution containing (in mM) 150 NaCl, 5 KCl, 2 $CaCl_2$, 2 $MgCl_2$, 10 glucose, and 10 Hepes (pH 7.3, adjusted with NaOH). Membrane currents were recorded at a −45 mV membrane potential using an Axopatch 1D amplifier, and digitized at 5–10 kHz by means of a Digidata 1332A data-acquisition system (Axon Instruments). Pipettes made from borosilicate glass with a 1.5-mm outer diameter (Narishige) were filled with a solution containing (in mM) 130 CsCl, 2 $MgCl_2$, 0.5 EGTA, 3 $Mg(ATP)_2$, 0.4 GTP, and 10 Hepes (pH 7.2, adjusted with CsOH).

Glycine was dissolved in the bath solution and rapidly applied to the cells. The EC_{50} value and Hill coefficient (n) for glycine-activated currents in individual cells were calculated by fitting data using a non-linear least-squares algorithm to the Hill equation: $I/I_{max} = [G]^n/(EC_{50}^n + [G]^n)$, where I is the magnitude of the peak current elicited by a concentration [G] of glycine, and I_{max} is the magnitude of the maximum peak current elicited by a saturating concentration of glycine. The data were fitted using KyPlot software (Kyence).

Statistical analysis. Data are presented as means ± SEM. A two-tailed unpaired Student's t test was used, with statistical significance set at $p < 0.05$.

Results

Cloning of a novel cDNA

Both a truncated splicing variant of GlyRα1 (GlyRα1^{del}: GenBank Accession No. AY827463) and full-length GlyRα1 (GlyRα1WT: GenBank Accession No. D00833) were cloned from adult rat brain cDNA. Fig. 1A shows the deduced amino acid sequence alignment for GlyRα1WT, GlyRα1^{del}, and GlyRα1^{ins} (which was reported by Malosio et al. [13]). The present deletion does not cause a frame shift, and GlyRα1^{del} lacked a part of the cytoplasmic loop between transmembrane regions TM3 and TM4. A comparison of the cDNA sequence with the rat genome (GenBank Accession No. NW042655) indicated that this cDNA clone contains a truncated exon 9 with a different acceptor site from those in GlyRα1WT and GlyRα1^{ins} (Fig. 1B).

Immunoblots of cell extracts of COS-7 cells transiently transfected with constructs tagged with Flag epitope revealed that, as expected, GlyRα1^{del} was capable of expression in such cells, and that its molecular weight was ~3 kDa lower than that of GlyRα1WT (Fig. 2A). When the cDNA for GlyRα1^{del} was expressed in COS-7 cells, immunofluorescence analysis showed that the GlyRα1^{del} was present in the cytoplasmic region, in which membrane proteins have previously been observed [14] (Fig. 2B). Similar results were obtained for GlyRα1WT (data not shown).

Functional expression of GlyRα1^{del} in HEK293 cells

To explore the functional properties of GlyRα1^{del}, cDNAs were expressed in HEK293 cells (because heterologous expression of the homomeric GlyRα1 in HEK293 cells generates glycine-gated chloride currents [15]). Whole-cell current responses were of similar magnitude for GlyRα1^{del} and GlyRα1WT (Fig. 3A and Table 1). The concentration-dependence of the whole-cell current amplitude gave similar values for the Hill coefficient, but significantly different EC_{50} values between the two channels (Fig. 3B and Table 1).

Next, the voltage was stepped from −60 to 20 mV at 10 mV intervals while isometric Cl^- and glycine were ap-

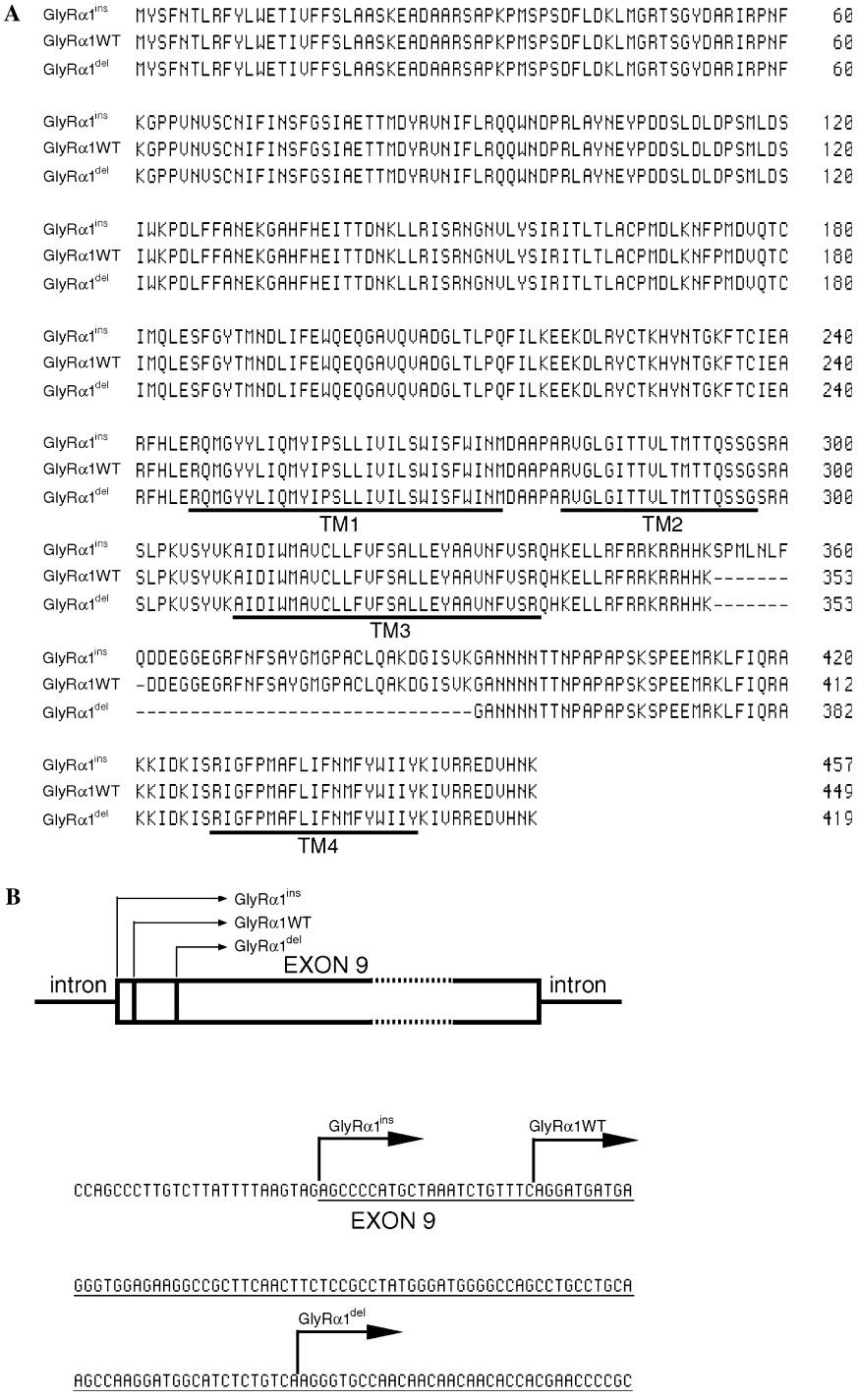

Fig. 1. Sequence analysis of rat GlyRα1 variants. (A) Alignment of proteins potentially translated from the truncated rat GlyRα1 (GlyRα1^{del}) subunit mRNA, compared to the wild-type (GlyRα1WT) and an inserted variant (GlyRα1^{ins}). The four putative transmembrane domains (TM1–TM4) are underlined. (B) Sequence around the border of the acceptor site of exon 9 of rat GlyRα1 derivatives. Each arrow shows an acceptor site in exon 9 within the indicated splicing variant of GlyRα1. The sequence in exon 9 of GlyRα1^{ins} is underlined.

plied to GlyRα1 derivative-expressing cells. For each receptor, the current reversed polarity at around 0 mV (GlyRα1WT, 3.9 ± 3.7 mV, $n = 4$; GlyRα1^{del}, -1.3 ± 4.3 mV, $n = 4$; Fig. 4), and there was no significant difference between these values ($p = 0.20$). The above values are similar to the theoretical reversal potential of Cl^- (−5.8 mV), suggesting that the expressed GlyRα1s function as Cl^- channels. Furthermore, over the range −60 to 20 mV, a similar linearity was observed in the two current–voltage relationships (Fig. 4).

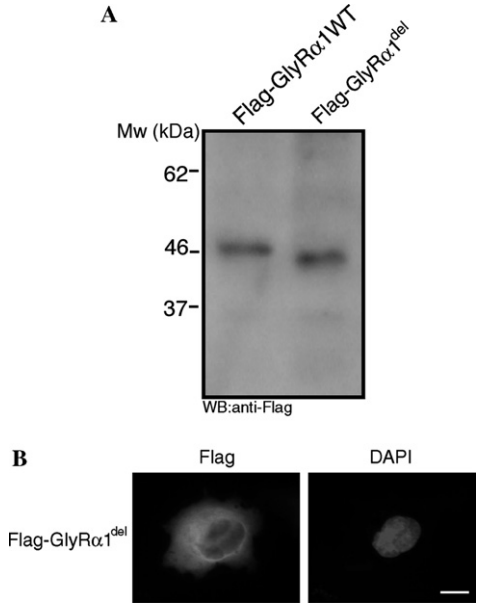

Fig. 2. Biochemical and immunocytochemical features of GlyRα1^{del}. (A) Immunoblot of Flag-tagged GlyRα1WT and GlyRα1^{del} expressed in COS-7 cells. Total cell lysates from COS-7 cells were resolved by 15% SDS–PAGE and then processed for immunoblotting with anti-Flag antibody. (B) Localization of Flag-tagged GlyRα1^{del} recombinant protein. COS-7 cells were transiently transfected with Flag-tagged GlyRα1^{del} expression vector for 24 h, stained using anti-Flag antibody and DAPI for nuclear staining, and then observed under the fluorescence microscope. Similar results were obtained from Flag-GlyRα1WT-expressing cells (data not shown). Scale bar, 25 μm.

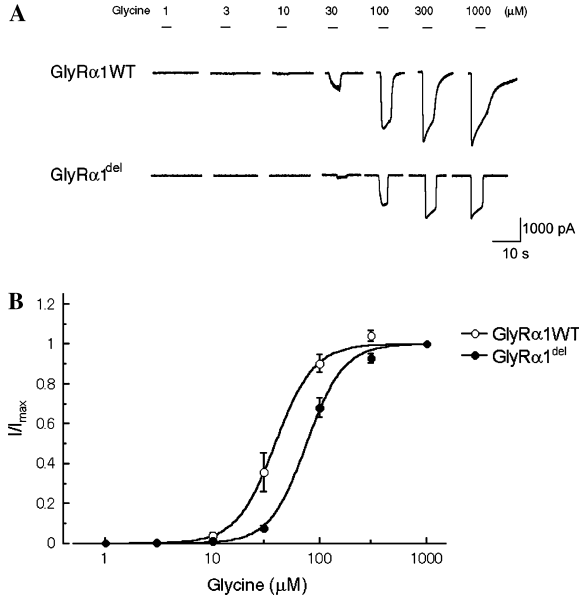

Fig. 3. Dose–response characteristics of GlyRα1WT and GlyRα1^{del}. (A) Concentration-dependence of glycine-induced whole-cell currents in HEK293 cells transiently transfected with GlyRα1WT or GlyRα1^{del}. Numbers above traces denote glycine concentration in micromolar. Membrane potentials were held at −45 mV. (B) Dose–response curves for GlyRα1WT and GlyRα1^{del}. Peak currents were normalized to the value obtained using 1000 μM glycine. Open and closed symbols correspond to GlyRα1WT ($n = 6$) and GlyRα1^{del} ($n = 9$) channels, respectively. Values are means ± SEM.

Table 1
Functional properties of GlyRα1 derivatives

Subunit	EC_{50} (μM)	n	Maximal response (pA)	No. of cells
GluRα1WT	43.3 ± 7.5	2.7 ± 0.2	2720 ± 210	6
GlyRα1^{del}	71.5 ± 3.4	2.8 ± 0.1	2190 ± 240	9

The sigmoid dose–response curves in Fig. 3B were fitted to the Hill equation, $I/I_{max} = [G]^n/([G]^n + EC_{50}^n)$, where I/I_{max} represents normalized current, EC_{50} is the glycine concentration eliciting a half-maximal response, [G] is the glycine concentration, and n is the Hill coefficient. Values are means ± SEM. The EC_{50} values are significantly different ($p = 0.002$).

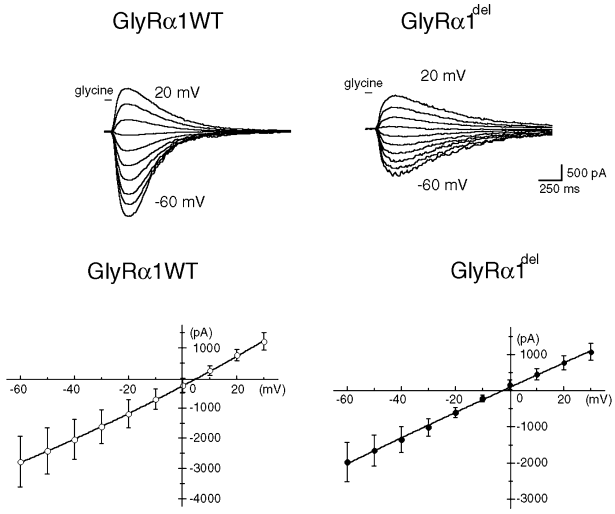

Fig. 4. Current–voltage plots for glycine currents. Representative traces and current–voltage plots of whole-cell currents recorded over the voltage range −60 to 20 mV from GlyRα1WT- and GlyRα1^{del}-expressing cells. Traces show typical currents induced by 100 μM glycine application. The reversal potentials (GlyRα1WT, 3.9 ± 3.7 mV, $n = 4$ vs GlyRα1^{del}, −1.3 ± 4.3 mV, $n = 4$; p value = 0.20) and the non-rectifying profiles were similar between the two channels. Values are means ± SEM.

Blocking by some GlyR antagonists

Several blockers are known for GlyRs. When glycine at 100 μM was applied to GlyRα1^{del}-expressing cells after preincubation with 1 μM strychnine, a GlyR blocker, glycine-induced currents were blocked almost completely (Fig. 5A). The dose-dependent blocking effects of strychnine were similar between GlyRα1WT and GlyRα1^{del} (Fig. 5B). Other GlyR antagonists, picrotoxin and picrotoxinin (each at 100 μM), also inhibited the GlyRα1^{del}-mediated current (Fig. 5B).

Discussion

In the present paper, we first revealed the existence of another truncated splicing variant of GlyRα1 in adult

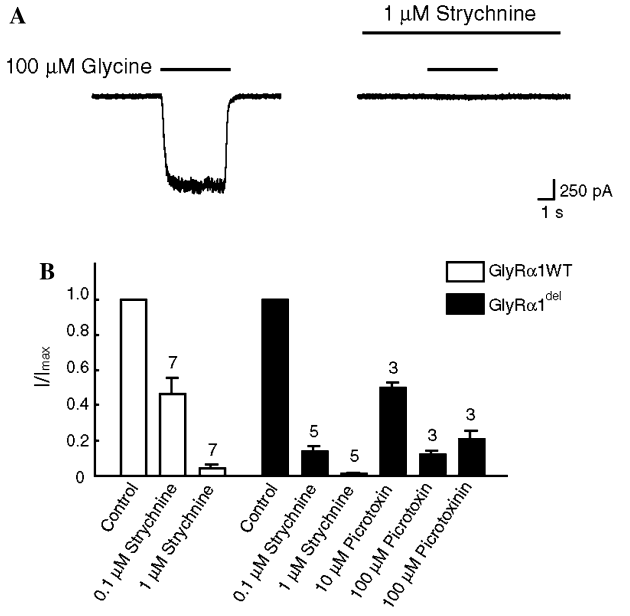

Fig. 5. Effects of glycine-receptor blockers on recombinant GlyRα1 derivatives. (A) Strychnine-sensitivity of GlyRα1^{del}. Glycine-induced currents were recorded in GlyRα1^{del}-expressing cells with (right) or without (left) 1 μM strychnine. Strychnine was applied 30 s before application of glycine. (B) Pharmacological properties of GlyRα1 derivatives. Glycine (100 μM)-induced currents were recorded in GlyRα1WT- or GlyRα1^{del}-expressing cells in the presence of various glycine-receptor antagonists as indicated. Values are means ± SEM (number of experiments is indicated above each column).

rat brain, and we functionally expressed it in HEK293 cells. The mRNA of the truncated form has a backward-transferred acceptor site in exon 9, resulting in a 30 a.a. deletion of the GlyRα1WT sequence. A previously reported GlyRα1 splicing variant, GlyRα1^{ins}, is also known to have an altered acceptor site in exon 9 [13], suggesting that this site may be an easy target for alternative splicing. This might be applicable to other members of the superfamily, because a similar event has been reported for both GlyRα3 and 5-HT$_3$ receptors [16,17]. In some members of the superfamily, such as acetylcholine receptors, the region between TM3 and TM4 is thought to play an important role in the intracellular regulation of the receptor. In GlyRα1, this region contains the site phosphorylated by protein kinase C, which modulates its function. Although the directly phosphorylated site is not involved in the area deleted from GlyRα1^{del}, the absence of this region might change the effect of the modulation. In addition, other type of modulation could be affected by the deletion because the channel properties of GlyRα1 can be modulated by both PKA and G-protein [18,19].

The α-subunits of GlyRs form functional homomeric channels in culture cells and/or *Xenopus* oocytes [18]. In the present study, we observed that GlyRα1^{del} is functional since it generated current upon activation by glycine. Under our conditions, both the peak amplitude and the Hill coefficient of GlyRα1^{del} were comparable to those obtained for GlyRα1WT, while the EC_{50} of the former was significantly higher. Similar results have been obtained for GlyRα3, in which the short form showed a left-shifted EC_{50} value when compared with the longer form [20].

Unfortunately, we were not able to explore the regional distribution of GlyRα1^{del}. Rat brains were separated into several parts, and RT-PCR was performed to detect GlyRα1s. However, the mRNAs for GlyRα1^{del} and GlyRα1^{ins} were not detected in any region (data not shown). This suggests that these isoforms may be present in only small amount in rat brain. The specific role played by GlyRα1^{del} within the nervous system remains to be explored.

Acknowledgments

We thank Dr. R. Timms for language editing the manuscript. This work was supported by a Grant-in-Aid for a Center of Excellence (COE), by Grant-in-Aid for Scientific Research on Priority Areas-Advanced Brain Science Project #16015252 from the Ministry of Education, Culture, Sports, Science and Technology, Japan, and by Grant-in-Aid for Scientific Research #16390058 from the Japan Society for the Promotion of Science (to A.F.).

References

[1] J.F. Leite, M. Cascio, Structure of ligand-gated ion channels: critical assessment of biochemical data supports novel topology, Mol. Cell. Neurosci. 17 (2001) 777–792.
[2] T.J. Jentsch, V. Stein, F. Weinreich, A.A. Zdebik, Molecular structure and physiological function of chloride channels, Physiol. Rev. 82 (2002) 503–568.
[3] W. Hoch, H. Betz, C.-M. Becker, Primary cultures of mouse spinal cord express the neonatal isoform of the inhibitory glycine receptor, Neuron 3 (1989) 339–348.
[4] H. Akagi, H. Hirai, F. Hishinuma, Cloning of a glycine receptor subtype expressed in rat brain and spinal cord during a specific period of neuronal development, FEBS Lett. 281 (1991) 160–166.
[5] B. Laube, G. Maksay, R. Schemm, H. Betz, Modulation of glycine receptor function: a novel approach for therapeutic intervention at inhibitory synapses? Trends Pharmacol. Sci. 23 (2002) 519–527.
[6] G. Grenningloh, A. Rientz, B. Schmitt, C. Methfessel, M. Zensen, K. Beyreuther, E.D. Gundelfinger, H. Betz, The strychnine-binding subunit of the glycine receptor shows homology with nicotinic acetylcholine receptors, Nature 328 (1987) 215–220.
[7] S. Rajendra, J.W. Lynch, K.D. Pierce, C.R. French, P.H. Peter, P.R. Schofield, Startle disease mutations reduce the agonist sensitivity of the human inhibitory glycine receptor, J. Biol. Chem. 269 (1994) 18739–18742.
[8] L. Zhou, K.L. Chillag, M.A. Nigro, Hyperekplexia: a treatable neurogenetic disease, Brain Dev. 24 (2004) 669–674.
[9] Z. Qu, E.D. Appel, C.A. Doherty, P.W. Hoffman, J.P. Merlie, R.L. Huganir, The synapse-associated protein rapsyn regulates tyrosine phosphorylation of proteins colocalized at nicotinic

acetylcholine receptor clusters, Mol. Cell. Neurosci. 8 (1996) 171–184.
[10] D.J. Glass, G.D. Yancopoulos, Sequential roles of agrin, MuSK, and rapsyn during neuromuscular junction formation, Curr. Opin. Neurobiol. 7 (1997) 379–384.
[11] G. Meyer, J. Kirsch, H. Betz, D. Langosch, Identification of a gephyrin binding motif on the glycine receptor β subunit, Neuron 15 (1995) 563–572.
[12] A. Luiz-Gomez, M.L. Vaello, F. Valdivieso, F. Mayor Jr., Phosphorylation of the 48-kDa subunit of the glycine receptor by protein kinase C, J. Biol. Chem. 266 (1991) 559–561.
[13] M.-L. Malosio, G. Grenningloh, J. Kuhse, V. Schmieden, B. Schmitt, P. Prior, H. Betz, Alternative splicing generates two variants of the α1 subunit of the inhibitory glycine receptor, J. Biol. Chem. 266 (1991) 2048–2053.
[14] J. Kirsch, J. Kuhse, H. Betz, Targeting of glycine receptor subunits to gephyrin-rich domains in transfected human embryonic kidney cells, Mol. Cell. Neurosci. 6 (1995) 450–461.
[15] I. Pribilla, T. Takagi, D. Langosch, J. Bormann, H. Betz, The atypical M2 segment of the β subunit confers picrotoxinin resistance to inhibitory glycine receptor channels, EMBO J. 11 (1992) 4305–4311.
[16] P. Uetz, F. Abdelatty, A. Villarroel, G. Rappold, B. Weiss, M. Koenen, Organisation of the murine 5-HT_3 receptor gene and assignment to human chromosome II, FEBS Lett. 339 (1994) 302–306.
[17] Z. Nikolic, B. Laube, R.G. Weber, P. Lichter, P. Kioschis, A. Poustka, C. Muelhardt, C.-M. Becker, The human glycine receptor subunit α3, J. Biol. Chem. 273 (1998) 19708–19714.
[18] M.-L. Vaello, A. Ruiz-Gomez, J. Lerma, F. Mayor Jr., Modulation of inhibitory glycine receptors by phosphorylation by protein kinase C and cAMP-dependent protein kinase, J. Biol. Chem. 269 (1994) 2002–2008.
[19] F.E. Yevenes, R.W. Peoples, J. Tapia, J. Parodi, X. Soto, J. Olate, L.G. Aguayo, Modulation of glycine-activated ion channel function by G-protein by subunits, Nat. Neurosci. 6 (2003) 819–824.
[20] H.-G. Breitinger, G. Villmann, J. Rennert, D. Ballhausen, C.-M. Becker, Hydroxylated residues influence desensitization behaviour of recombinant α3 glycine receptor channels, J. Neurochem. 83 (2002) 30–36.